



# Chitosan/aloë vera gel coatings infused with orange peel essential oils for fruits preservation

Wen Xia Ling Felicia<sup>a</sup>, Rovina Kobun<sup>a,\*</sup>, Nasir Md Nur Aqilah<sup>a</sup>, Sylvester Mantihal<sup>a</sup>, Nurul Huda<sup>b</sup>

<sup>a</sup> Faculty of Food Science and Nutrition, Universiti Malaysia Sabah, Kota Kinabalu, Sabah, Malaysia

<sup>b</sup> Faculty of Sustainable Agriculture, Jalan Sg. Batang, Mile 10, UMS Sandakan Campus, 90000, Sandakan, Sabah, Malaysia

## ARTICLE INFO

Handling editor: Xing Chen

### Keywords:

Antibacterial activity  
Antioxidant activity  
Particle size  
Orange peel essential oil  
Polysaccharides  
Fruit coating technology

## ABSTRACT

Continuous fruit waste poses significant environmental and economic challenges, necessitating innovative fruit coating technologies. This research focuses on harnessing discarded orange peels to extract essential oil (OPEO), which is then integrated into a chitosan/aloë vera (CTS/AVG) matrix. The study comprehensively characterised the coating in terms of its physicochemical properties, antioxidant capacity, and antimicrobial efficacy. The investigation involved an analysis of particle size and distribution in the coating solutions, highlighting changes induced by the incorporation of orange peel essential oil (1 %, 2 % and 3 % v/w) into the chitosan/aloë vera (4:1 v/v) matrix, including particle size reduction and enhanced Brownian motion. The study quantifies a 33.21 % decrease in water vapour transmission rate and a reduction in diffusion coefficient from  $9.26 \times 10^{-11} \text{ m}^2/\text{s}$  to  $6.20 \times 10^{-11} \text{ m}^2/\text{s}$  following the addition of OPEO to CTS/AVG. Assessment of antioxidant potential employing DPPH radical scavenging assays, revealed that CTS/AVG/3 %OPEO exhibited notably superior radical scavenging activity compared to CTS/AVG, CTS/AVG/1 %OPEO, and CTS/AVG/2 %OPEO, demonstrated by its  $\text{IC}_{50}$  value of  $17.01 \pm 0.45 \text{ mg/mL}$ . The study employs the well diffusion method, demonstrating a higher susceptibility of gram-negative bacteria to the coating solutions than gram-positive counterparts. Remarkably, CTS/AVG/3 %OPEO displayed the most pronounced inhibition against *Escherichia coli*, generating an inhibitory zone diameter of  $14 \pm 0.8 \text{ mm}$ . The results collectively emphasised the potential of CTS/AVG/3 %OPEO as a viable natural alternative to synthetic preservatives within the fruit industry, attributed to its exceptional antioxidant and antimicrobial properties.

## 1. Introduction

Recently, polymer-based packaging systems that prolong the shelf life of food have garnered attention from researchers and companies alike due to their unique properties of biodegradability and environmentally friendly food packaging system (Panda et al., 2022). People have always been interested in packaging materials such as low-density polyethylene due to their versatility, flexibility, durability and good mechanical properties (Diyana et al., 2021). However, some drawbacks of plastics, such as the migration effect occurring within the foods during storage and their non-biodegradability, have caused a growing global awareness and posed adverse health effects to consumers and the environment (Azman et al., 2021). Edible coatings, biopolymer-based packaging materials composing of polysaccharides, proteins, and

lipids, provide numerous advantages as an alternative to non-biodegradable plastics, including providing protection to food products by acting as a barrier to external conditions, prolonging shelf life, sustaining the food quality, and are environmentally friendly packaging (Felicia et al., 2022a,b).

Chitosan, a chitin derivative, a cationic polysaccharide composed of N-acetyl glucosamine and D-glucosamine, has been acknowledged as a versatile biopolymer with its biodegradability, biocompatibility, non-toxicity and low allergenicity. Chitosan has been demonstrated to suppress growth of pathogenic microorganisms and improve self-life due to the presence of its reactive groups (Duan et al., 2019). Literature reveals that incorporation of aloë vera in chitosan forming a biodegradable coating can improve the functionalities of the packaging system (De Matteis et al., 2023). In a previous study, chitosan coating was used to

Abbreviations: AVG, Aloë vera gel; CTS, Chitosan; OPEO, Orange peel essential oil.

\* Corresponding author.

E-mail address: [rovinaruby@ums.edu.my](mailto:rovinaruby@ums.edu.my) (R. Kobun).

<https://doi.org/10.1016/j.crfs.2024.100680>

Received 25 September 2023; Received in revised form 30 December 2023; Accepted 12 January 2024

Available online 1 February 2024

2665-9271/© 2024 Published by Elsevier B.V. This is an open access article under the CC BY-NC-ND license (<http://creativecommons.org/licenses/by-nc-nd/4.0/>).

successfully extend the storage life of several fruits, including 'Galia' melons and 'Gala' apples (Shebis et al., 2022), cantaloupe (Qiao et al., 2019), and banana (La et al., 2021). Similarly, aloe vera gel has been demonstrated to have antimicrobial treatment for various fruit pathogens (Esmaeili et al., 2021). Several fruits have been successfully preserved by using aloe vera gel as an edible coating, including apricots (Nourozi and Sayyari, 2020), plums (Ali et al., 2021), and strawberry (Liguori et al., 2021). Currently, researchers are interested in the combined impact of edible coatings on fruit postharvest diseases.

Furthermore, incorporating essential oil, a concentrated hydrophobic liquid derived from aromatic plants, into edible packaging has become the current trend in the research field of food packaging as it has been reported to have a great number of bioactive components such as phenolics and terpenoids. OPEO was chosen due to its remarkable antimicrobial and antioxidant properties, attributed to its rich chemical composition, particularly high levels of limonene and  $\beta$ -myrcene (Akarca and Sevik, 2021). The literature review has highlighted gaps in the utilisation of OPEO in food packaging materials, particularly the need for a more comprehensive exploration of its potential. It is well documented that the incorporation of essential oils such as cinnamon, thyme, lemongrass and garlic oil into the chitosan/aloe vera matrix can produce active packaging (Alkaabi et al., 2022).

To the best of our knowledge, there is no literature related to incorporation of orange peel essential oil (OPEO) in the chitosan/aloe vera matrix and their characterisation. In this study, we aimed to characterise the physicochemical properties of chitosan/aloe vera gel coatings incorporated with orange peel essential oil including particle size analysis, emulsion stability, viscosity, pH and density, water vapour transmission rate, diffusion coefficients, UV-Vis shielding, colour, FTIR analysis, as well as antioxidant and antibacterial activity, with the goal of understanding the potential of this coating system for extending the shelf life of fresh and minimally processed foods.

## 2. Material and methods

### 2.1. Raw materials

Orange peel waste was collected from Boost, 1 Borneo, Kota Kinabalu, Sabah. Fresh aloe vera leaves were harvested from the cultivated aloe vera plants in the Faculty of Food Science and Nutrition, Universiti Malaysia Sabah. Chitosan powder, from shrimp shells ( $\geq 75\%$  deacetylation) was purchased from Sigma-Aldrich. Acetic acid,  $\text{CH}_3\text{COOH}$ , was purchased from System Chemicals.

### 2.2. Preparation of coating solution

1 % chitosan solution (w/v) was prepared through dissolution of 1 g of chitosan in 100 mL solution containing 2 % acetic acid (v/v) (Pavoni et al., 2019). Aloe vera leaves were thoroughly washed to remove any dirty debris or surface contaminants. The outer green rind of the aloe vera leaves were cut using a clean, sharp knife and the aloe vera gel was scooped out using a spoon. It was then blended and homogenised in a blender and filtered using a strainer with mesh size of 125- $\mu\text{m}$  particle size to remove any impurities. Chitosan/aloe vera coating solution was prepared in the ratio of 4:1 (v/v) (Amin et al., 2021). The orange peel fruits were cleaned, dried in a 65 °C universal oven (Stericell 222, United States) for 4 h, and ground into a powder with a 125- $\mu\text{m}$  particle size and a moisture content of  $10.28 \pm 1.19\%$ . The dried powdered orange peels were utilised to extract the essential oil using a Soxhlet extractor (Borosil, India) A rotary evaporator (Heidolph, Schwabach, Germany) with a temperature of 60 °C was used to remove ethanol to obtain the essential oil. A sealed vial containing the extracted essential oil was transferred and kept at 4 °C. Afterward, different concentrations of orange peel essential oil (1 %, 2 % and 3 % v/v) was added in the chitosan/aloe vera solution.

### 2.3. Characterization of coating solutions

#### 2.3.1. Particle size analysis

The particle size of coating solutions were determined using the particle size analyser (Particulate Systems, NanoPlus Zeta/Nano Particle Size, USA) by means of dynamic light scattering (DLS) principle. The sample was diluted in ethanol with a dilution factor of 10 and homogenised prior to analysis. The instrument was set up by selecting the measurement mode and setting the measurement parameters in SOP Designer. The microvolume cell was then filled with the diluted essential oil, and the measurement was initiated. The samples were performed at 25 °C with the detection angle of 90° and refractive index of 1.36 (Peng and Li, 2014).

#### 2.3.2. Emulsion stability

Emulsion stability was determined using a modified version of the approach described by Amin et al. (2021). 3 mL of each coating formulation was placed in a test tube and exposed to ambient conditions for three days. The emulsion stability was determined using equation (1):

$$\text{Emulsion stability} = \frac{h_o - h_t}{h_o} \quad \text{Equation 1}$$

where  $h_o$  and  $h_t$  is the initial and final height of the emulsion in the test tube after three days of storage, respectively.

#### 2.3.3. Determination of viscosity, pH and density

Viscosity of the coating solutions was determined using a rotational viscometer (RVDV-II + P Brookfield, USA) equipped with a DV-2+ RV Pro RV spindle. The viscosity of the coating solutions was evaluated at  $T = 20$  °C with spindle size range from 0.2 to 0.7 (Lastra Ripoll et al., 2021). Meanwhile, pH of coating solutions was determined at room temperature using a pH metre (Eutech 2700, Singapore). The pH metre was calibrated using standard buffers with pH value of 4 and 7. Furthermore, the density of the coating solution was evaluated by weighing and recording the weight of a 10 mL beaker. Following that, 5 mL of coating solutions were added into the beaker and the weight was determined. Equation below was used to measure the density of the coating solutions.

$$\text{Density of coating solution} = \frac{\text{Weight of the sample (g)}}{\text{Volume of the sample (mL)}} \times 100 \quad \text{Equation 2}$$

#### 2.3.4. Water vapour transmission rate (WVTR)

The WVTR of the coatings were determined using the ASTM technique (ASTM, 2013) with minor changes. Coating solutions were casted into films and dried at  $23 \pm 2$  °C on a Petri dish with diameter of 90 mm until the coating solutions form a thin sheet or films. Glass tubes (2 × 5 cm) were filled with desiccant (silica gel) and dried films were applied to the tube's face (by using gel). The films were kept at  $38 \pm 0.6$  °C in an incubator. The weight of the tubes were tested on a regular basis for four weeks to determine the WVTR. The following equation was used to compute WVTR:

$$\text{WVTR} = \frac{\Delta m \times T}{A \times t \times \Delta P} \quad \text{Equation 3}$$

Here,  $\Delta m$  is the change in mass (g) before and after the specific time,  $A$  is the area ( $\text{m}^2$ ),  $t$  is the time (hours),  $T$  is the thickness of films and  $\Delta P$  is the difference in pressure at saturated pressure and pressure under the testing conditions.

#### 2.3.5. Diffusion coefficient

Fick's law of diffusion was used to calculate the moisture loss in terms of diffusion through the coatings:

$$MR = \frac{M_t - M_e}{M_0 - M_e} = \frac{8}{\pi^2} \exp\left(\frac{-\pi^2 Dt}{4L^2}\right)$$

In this equation, MR, D, t and L represent the moisture ratio, effective diffusion coefficient ( $\text{m}^2/\text{s}$ ), time (s) and thickness (m) of the sample layer, respectively. Additionally,  $M_t$ ,  $M_e$ ,  $M_0$  represent moisture levels at time intervals of t, initial and equilibrium, respectively. The diffusion coefficient can be derived from the slope of line ( $\alpha$ ) drawn between  $\ln(MR)$  and time as (Amin et al., 2021):

$$\alpha = \left(\frac{\pi^2 Dt}{4L^2}\right) \quad \text{Equation 4}$$

### 2.3.6. UV-Vis shielding

The UV-transmittance was measured using PerkinElmer Lambda 35 UV-Vis scanning spectrophotometer and the light absorption spectrum of the coating solutions were obtained in the range of 200–800 nm.

### 2.3.7. Colour

Colour values of coating solutions were evaluated using a colourimeter (ColourFlex, HunterLab, United Kingdom) and documented in terms of  $L^*$  (brightness),  $a^*$  (from redness to greenness) and  $b^*$  (from yellowness to blueness). Using Equation (5), the total colour difference ( $\Delta E$ ) can be calculated using the obtained values of  $L^*$ ,  $a^*$  and  $b^*$ , which represents the colour saturation of the coating solutions. Values were determined as the average of three measurements of each coating solution (Li et al., 2021).

$$\Delta E = [(L^*-L)^2 + (a^*-a)^2 + (b^*-b)^2]^{1/2} \quad \text{Equation 5}$$

where,  $L^*(93.87)$ ,  $a^*(-0.73)$  and  $b^*(2.06)$  were the standard colour parameters of the calibration plate.

### 2.3.8. FTIR analysis

FTIR spectrometer (Agilent Technologies, USA) analysis of the coating solutions was performed. Using the absorbance mode, the spectra were obtained between 4000 and 650  $\text{cm}^{-1}$  with a resolution of 4  $\text{cm}^{-1}$  (Sheikh et al., 2021).

### 2.3.9. Antioxidant activity

A 1,1-diphenyl-2-picrylhydrazyl (DPPH) radical scavenging assay was used to evaluate the free radical scavenging activity of various coating solutions. 3 mL of a 0.1 mM DPPH solution was combined with 1 mL of the tested compounds dissolved in ethanol at various concentrations (40, 80, 120, 160, 200 mg/mL) prepared by sequential dilution. At room temperature of 22 °C, the mixture was agitated for 30 min; then, the absorbance of the reaction mixture was measured at 517 nm using a spectrophotometer (UV-VIS PerkinElmer Lambda 35). Using a log dose inhibition curve, the dose of tested compounds required to inhibit 50 % of the DPPH free radical ( $\text{IC}_{50}$ ) was determined. Ascorbic acid was utilised as the standard antioxidant agent.

$$\text{Efficacy of DPPH scavenging (\%)} = \frac{CA - TCA}{CA} \times 100 \quad \text{Equation 6}$$

where CA and TCA are the absorbance of the control reaction and tested compound reaction, respectively.

### 2.3.10. Antibacterial activity

Antibacterial activity of coating solutions were determined using the well diffusion method. 3.5 g/100 mL of Mueller Hinton agar was dissolved in hot distilled water and stirred well. The medium was sterilised using an autoclave at 121 °C for 15 min. The medium was transferred into sterilised petri dishes and were let hardened before 0.1 mL of inoculum was added to the medium. 7 mm wells were made with sterile pipette tips on the sterilised agar. The wells were loaded with different coating solutions, and nutrient broth as negative control while

antibiotics disc as positive control. The petri dishes were incubated at 38 °C for 24 h. After 24 h, the antibacterial activity of the coating solutions were determined by measuring the inhibition zones around the well impregnated with the coating solutions (Sathiyaraj et al., 2021). According to Chowdhury et al. (2020), inhibition zone less than 5 mm is classified as no antibacterial activity, inhibition zone in the range of 6 mm–12 mm is classified as moderate antibacterial activity, and the inhibition zone exceeding 13 mm is classified as strong antibacterial activity.

## 2.4. Statistical analysis

All data was recorded as a mean  $\pm$  standard of deviation ( $n = 3$ ) using IBM SPSS Statistics v28.0. Data was analysed using a one-way ANOVA, followed by the Tukey Post-Hoc test. One-way ANOVA was performed using a 95 % confidence interval with  $p < 0.05$ , which illustrated a significant difference between samples.

## 3. Results and discussion

### 3.1. Particle size analyzer and emulsion stability

Figs. 1 and 2 depict the size and number distribution functions of coating solutions using the dynamic light scattering principle (Gupta et al., 2023). The versatility of this technique in terms of producing rapid, simple, reproducible, and non-destructive results for determining particle size is an advantage of its application. Time-dependent variations in the scattered light from a suspension of nanoparticles, as governed by their Brownian motion, are studied using dynamic light scattering (Jia et al., 2023).

Particle size and size distribution are the most crucial parameters of emulsions, dictating their properties such as rheology, appearance, and stability (Cirin et al., 2023). Figs. 1 and 2 illustrate the effect of OPEO concentration on the logarithmic distribution of particles in emulsions. In this context, several percentile values, including P1, D10, D50, and D90, are commonly used to characterise the size distribution. These values are determined by calculating the fraction of particles in the sample that are smaller than a given dimension. P1, D10, D50, and D90 refer to the particle diameters below which 1 %, 10 %, 50 %, and 90 % of the particles, respectively, are found.

In this investigation, it was discovered that the presence of OPEO affects the particles in coating solutions. According to our study, the addition of OPEO to chitosan/aloë vera gel (CTS/AVG) coating solution decreased the percentile values and cumulant diameter due to the presence of very fine OPEO particles. It can fill voids or interstitial spaces between CTS/AVG particles or act as spacer particles, preventing the agglomeration or clustering of CTS/AVG particles (Cheng et al., 2020). This method of dispersion may result in a more homogenous distribution of OPEO particles within the CTS/AVG matrix, thereby decreasing the average diameter of the coating particles. In addition, the incorporation of a greater concentration of OPEO in CTS/AVG coating solutions demonstrated a direct correlation with the propensity to endure Brownian motion. CTS/AVG/3 %OPEO has the smallest cumulant diameter at 998 nm, indicating that there is increased motion within the particles, resulting in increased collisions due to their size and mass (Soltani et al., 2022).

In addition, the cumulant diameter may provide insight into the size of the droplets distributed in the emulsion. In general, smaller and more homogenous droplet sizes contribute to enhanced emulsion stability by mitigating Ostwald ripening, creaming and sedimentation, and promote enhanced interfacial stability (Zheng and Rao, 2023). Therefore, emulsions remained stable for all OPEO concentrations after three days without phase separation and decrease in the height of the coating solutions. This indicates that OPEO is well dispersed in the CTS/AVG matrix. Differential number is a representation of the number of particles in a sample distributed across different size ranges or intervals. The

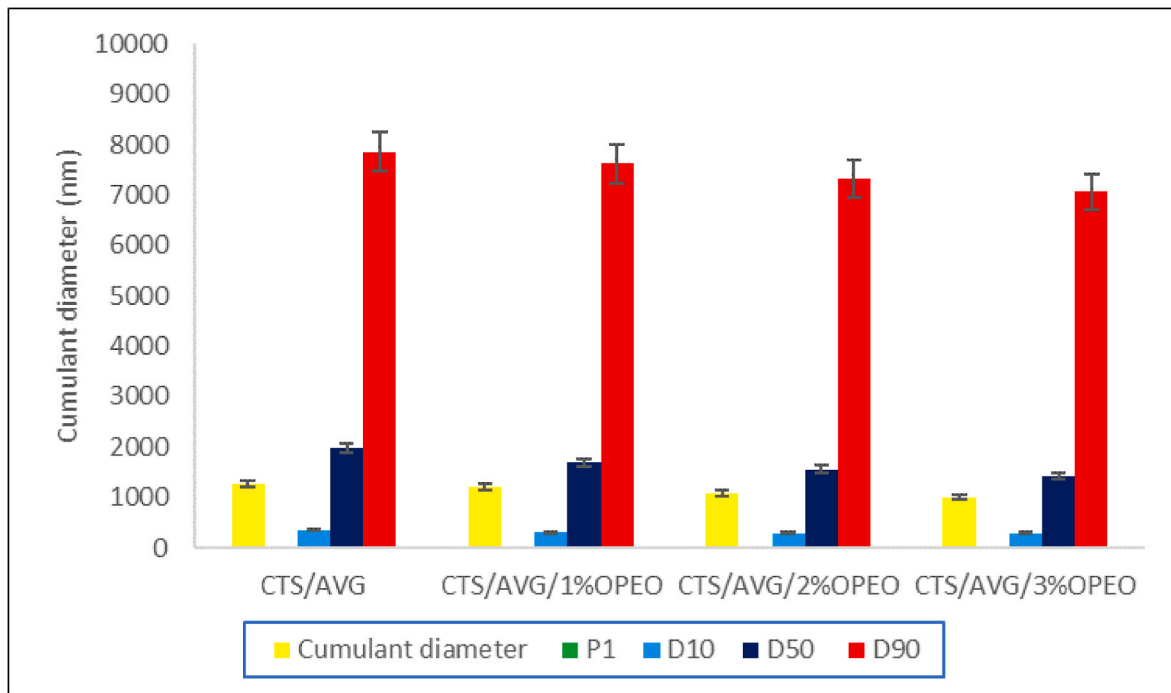


Fig. 1. Cumulant diameter of CTS/AVG, CTS/AVG/1 %OPEO, CTS/AVG/2 %OPEO, CTS/AVG/3 %OPEO.

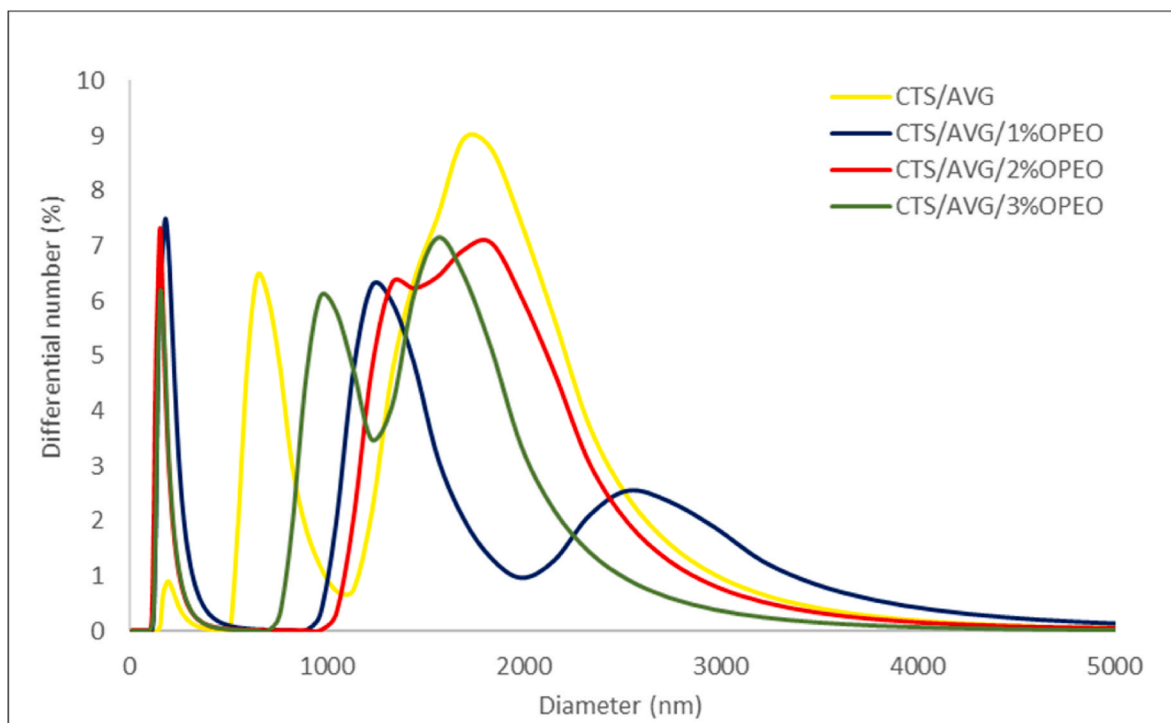


Fig. 2. Particle size distribution of CTS/AVG, CTS/AVG/1 %OPEO, CTS/AVG/2 %OPEO, CTS/AVG/3 %OPEO.

percentage of particles within various size intervals that are reactive relative to the total number of particles in the sample is depicted in Fig. 2. In general, a high percentage of the percentage differential number at large diameters would indicate a larger cumulant diameter. It suggests there is a sizable population of particles in the larger size range. CTS/AVG coating particles range from 1000 nm to 3000 nm, with the largest particles measured at 1693 nm and a differential number of 8.56 %. This can occur because of particle agglomeration or clustering, which

results in larger particle structures (Algharib et al., 2022). The addition of OPEO decreased both the diameter and the percentage of the differential number. Fig. 2 depicts a result that corresponds to the findings in Fig. 1.

### 3.2. Viscosity, pH and density

Chitosan, aloe vera gel, and orange peel essential oil are natural

ingredients that have gained attention for their potential use in various applications. When combined as a coating solution, the properties of the solution such as viscosity, pH, and density (Table 1) play a critical role in determining its effectiveness.

Chitosan, a natural biopolymer, forms gels in acids and forms good films (Wang and Zhuang, 2022). Meanwhile, AVG contains polysaccharides and other lubricants (Mohammadi et al., 2021). The CTS/AVG solution had the maximum viscosity of  $24.60 \pm 0.20$  cP, possibly due to its capacity to build a network of cross-linked polymer chains that impede liquid movement (Iqbal et al., 2023). OPEO contains terpenoids and other chemicals with various physiological effects. In this investigation, OPEO reduced viscosity in the CTS/AVG matrix, with the largest reduction at the highest concentration. This is likely because OPEO comprises chemicals that can disrupt the network of cross-linked polymer chains and improve fluidity by interfering with the hydrogen bonding and electrostatic interactions between CTS and AVG molecules (Ahmed et al., 2021).

Furthermore, Table 1 reveals that coating solutions influenced solution pH. The lowest pH was  $3.21 \pm 0.02$  for CTS/AVG/1 %OPEO and the highest was  $3.32 \pm 0.01$  for CTS/AVG/3 %OPEO. The pH of the CTS/AVG mixture decreased initially as OPEO concentration increased. This is notably due to the presence of several volatile aroma compounds in OPEO, most notably free fatty acids (TsegayeFekadu and Abera, 2019). However, as the concentration of OPEO increases, the pH values of the coating solutions change significantly ( $p < 0.05$ ). This is probably due to the buffering capacity of CTS/AVG that could counteract the acidic nature of OPEO components, thus neutralising the effects on pH. Chitosan contains amino groups which can exist in both protonated and deprotonated forms. As pH changes, the balance between these forms can act as a buffer, helping to resist significant shifts in pH (Ernesto et al., 2023). Additionally, AVG also contains various natural compounds, including amino acids, which can contribute to its buffering capacity due to its ionizable functional groups that can act as weak acids or bases, helping to maintain pH stability (Ajaz et al., 2023).

Density is a measure of mass per unit volume, and the data shows that the density values of the treatments are relatively similar, with a significant decrease in density observed as the concentration of OPEO increases. The lowest density value was observed in the CTS/AVG/3 %OPEO treatment, which indicates that the addition of OPEO can decrease the mass of the solution. This might be due to the presence of limonene, linalool, and citral, in OPEO which may interact with CTS/AVG coating solution to reduce density (Felicia et al., 2022a,b). OPEO may also lower CTS/AVG coating solution density because essential oils are less dense than water or gel-based substances, therefore, the addition of OPEO could displace some of the volume in CTS/AVG coating solution, resulting in a decrease in density. Moreover, when OPEO is added to the mixture, it may take further mixing or agitation to evenly distribute the oil, which could generate air bubbles or create pockets of lower density within the mixture, contributing to an overall decrease in density (Huang et al., 2021).

### 3.3. Water vapour transmission rate (WVTR) and diffusion coefficient

WVTR is the most crucial barrier attribute of packaging materials.

**Table 1**

The viscosity, pH and density of different coating solutions.

Treatments	Viscosity, cP	pH	Density, g/cm <sup>3</sup>
CTS/AVG	$24.60 \pm 0.20^a$	$3.27 \pm 0.04^{ab}$	$1.49 \pm 0.00^a$
CTS/AVG/1 %OPEO	$23.30 \pm 0.20^b$	$3.21 \pm 0.02^b$	$1.43 \pm 0.00^b$
CTS/AVG/2 %OPEO	$21.73 \pm 0.15^c$	$3.24 \pm 0.01^b$	$1.39 \pm 0.00^c$
CTS/AVG/3 %OPEO	$19.53 \pm 0.15^d$	$3.32 \pm 0.01^a$	$1.36 \pm 0.00^d$

<sup>2</sup> Values in the same column with different superscript letters are significantly different ( $p < 0.05$ ).

Values are stated as mean  $\pm$  standard deviation,  $n = 3$ .

WVTR of the packaging material should be enhanced to prevent the growth of bacteria and maintain the freshness of food. It needs to be resistant to polar water vapour in the coating barrier material, and it needs to be able to seal off pores and voids (Bhaskar et al., 2023).

WVTR denotes the permeability of a film or coating to restrict the movement of moisture from the atmosphere into the food products or vice versa (Azmin and Nor, 2020). Substantially, WVTR shows a direct effect on the performance of the film or coating to preserve the moisture contents of food (Mahajan et al., 2021). Result for water vapour permeability of films is shown in Fig. 3. The highest value of WVTR was observed for CTS/AVG coating solution and the lowest for CTS/AVG/3 %OPEO. Thus, increasing the concentration of OPEO resulted in 33.21 % reduction in water vapour permeability of films. Also calculated and depicted in Fig. 3 is the diffusion of moisture through the coating solutions. Increased OPEO concentration in the CTS/AVG matrix significantly reduced moisture diffusion through the coatings, as measured by the diffusion coefficient. Initially, moisture diffusion coefficient was observed to be  $9.26 \times 10^{-11}$  m<sup>2</sup>/s, which was reduced to  $6.20 \times 10^{-11}$  m<sup>2</sup>/s as the concentration of OPEO increased in the coating formulations. This is obvious due to the increased concentration of OPEO in the coating solutions.

Generally, the transfer of water vapour occurs via the hydrophilic segment of the barrier of the coating, and it is directly proportional to the ratio of hydrophilic to hydrophobic compounds. Therefore, introducing hydrophobic compounds such as OPEO decreases the moisture barrier (Nogueira et al., 2019). Chemical composition of essential oil plays a crucial role in edible film barrier properties (Mahcene et al., 2020). Principally, citrus fruits contain 90 % terpenes, 5 % oxygenated compounds and less than 1 % non-volatile compounds including waxes and pigments, as the main chemical compositions (Padilla-de la Rosa et al., 2021).

The hydrophobicity of the coating may be affected by the concentration of monoterpenes. Essentially, monoterpenes are the driving force for hydrophobicity. A hydrophobic disperse phase reduces water vapour transfer rate even at low ratios because it imposes an interfering hydrophilic phase (Hasheminya et al., 2019). Moreover, according to Amin et al. (2021), the presence of AVG reduced the water vapour transmission rate of the coating due to the high hydrophobicity of AVG. Addition of AVG to CTS will have synergistic interaction that causes better water barrier properties. Similar findings were reported by Mahajan et al. (2021) where addition of AVG reduced WVTR. Packaging plays a vital role in preserving and protecting the food from external atmosphere that might cause quality deterioration to the food.

### 3.4. UV-vis shielding

To limit the generation of free radicals, edible coatings should block the passage of UV light to food. Free radicals cause problems in food by disrupting antioxidants, lipids, vitamins, and proteins (Kohli et al., 2019). In addition to the destruction effect, senescence phenomena are detected, which causes a change in food colour and the development of off flavours. The UV shielding of CTS/AVG/OPEO coating solution is analysed and recorded over a UV and visible range of wavelengths (200–800 nm) as depicted in Figs. 4 and 5. One of the key elements affecting the quality of edible coating is its opacity.

Generally, the descending order of the UV light barrier properties of the coating solutions can be stated as follows: CTS/AVG/3 %OPEO > CTS/AVG/2 %OPEO > CTS/AVG/1 %OPEO > CTS/AVG. The UV blocking capabilities of CTS-containing solutions are mostly attributable to the presence of amino groups of N-acetylglucosamine and glucosamine residues. Meanwhile, the presence of phenolic groups in AVG might be the major compounds that absorb UV radiation. Additionally, the incorporation of OPEO further enhanced the UV shielding capacity of the coating solutions as it contains a more diverse range of terpenes (Bitterling et al., 2022). Strategically, UV shielding of the coating solutions majorly depends on the percentage of OPEO, as an increase in

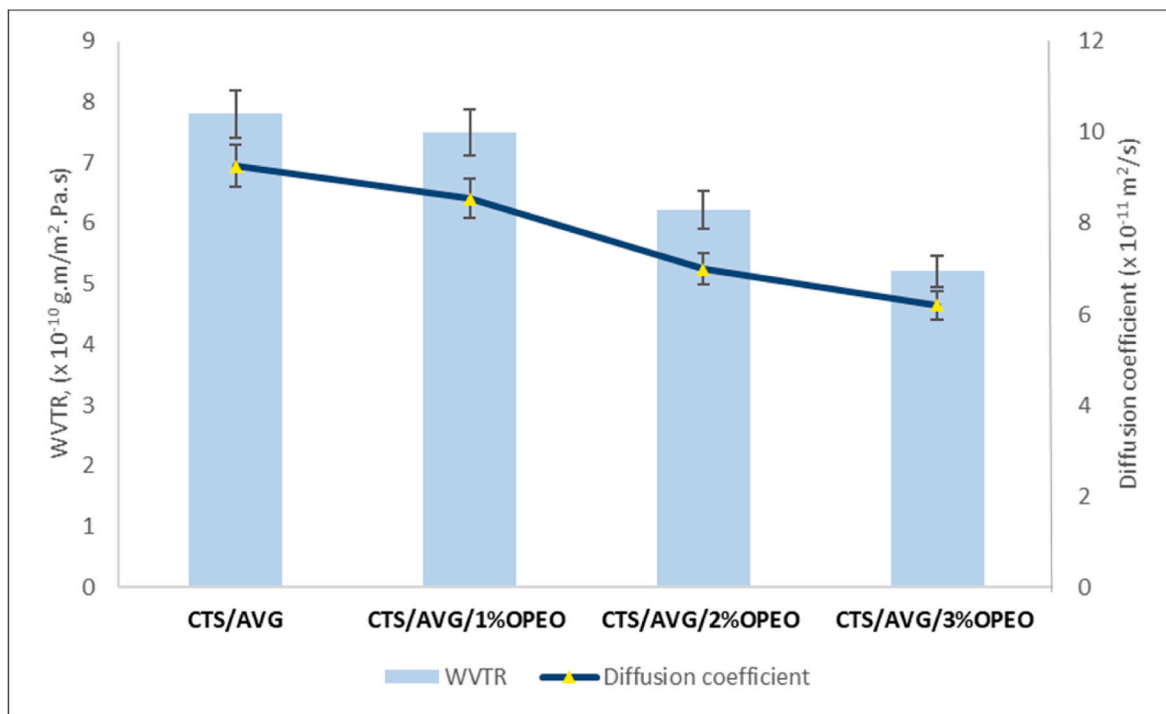


Fig. 3. Water vapour transmission rate and diffusion coefficient of CTS/AVG, CTS/AVG/1 %OPEO, CTS/AVG/2 %OPEO, CTS/AVG/3 %OPEO.

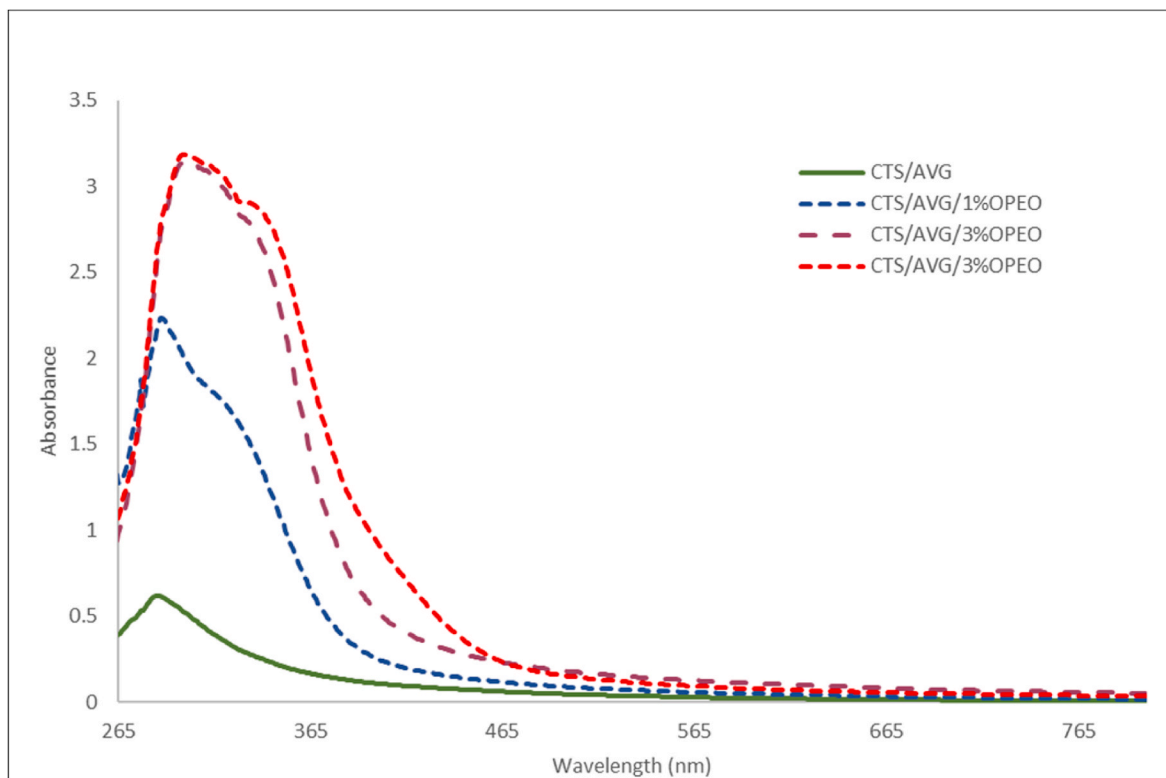


Fig. 4. Absorbance versus wavelength of CTS/AVG, CTS/AVG/1 %OPEO, CTS/AVG/2 %OPEO, CTS/AVG/3 %OPEO.

OPEO decreases the transparency of the coating solutions. CTS/AVG/3 %OPEO showed the lowest light transmittance among all the studied coating solutions at the UV region of 300 nm–400 nm, proving that the presence of OPEO would prevent light from passing through the coating solution. This could probably be due to the presence of the agglomerated molecular structure of OPEO causing light scattering at the interface of

incorporated essential oil droplets (Shen et al., 2021).

Besides, lower light transmittance might also be attributed by the coalescence effect and reflection by the lipid molecules localised in the coating solution. In addition, the inclusion of OPEO deepened the colour and might be one of the reasons for its low light transmittance. This finding agrees with previous studies in which transparency of

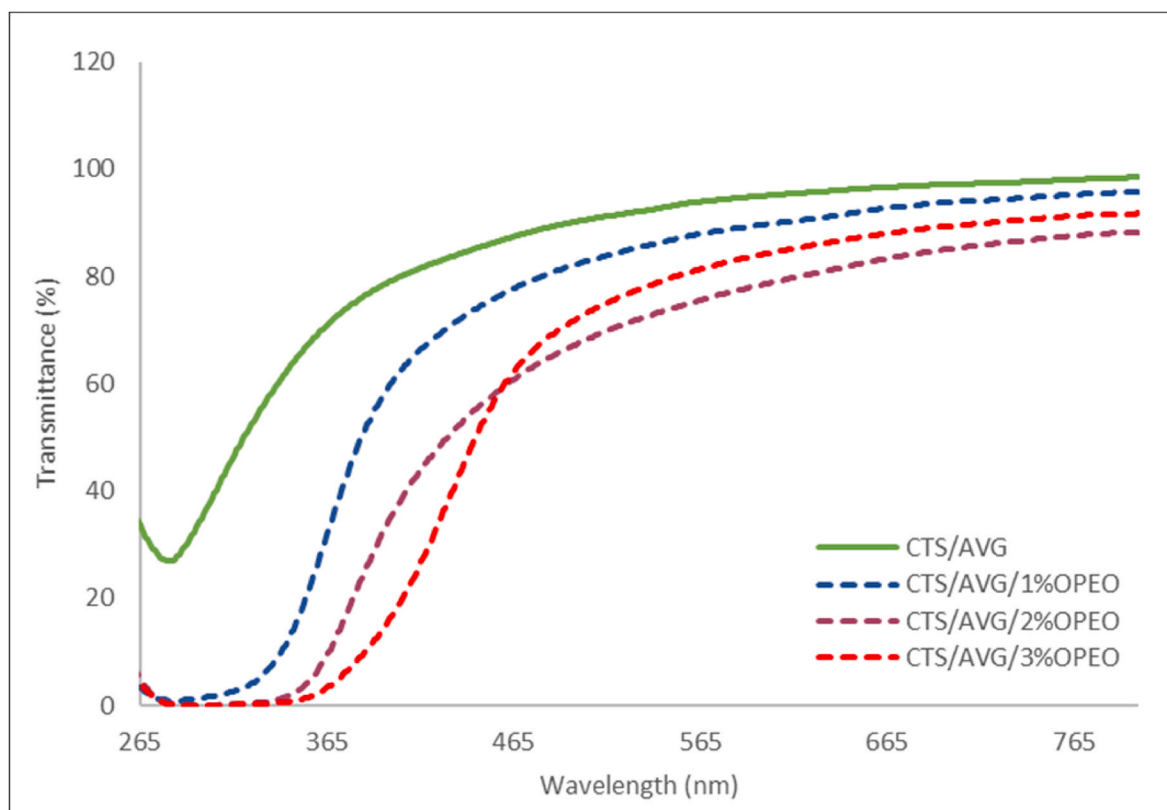


Fig. 5. Light transmittance versus wavelength of CTS/AVG, CTS/AVG/1 %OPEO, CTS/AVG/2 %OPEO, CTS/AVG/3 %OPEO.

hydroxypropyl methylcellulose and cassava starch film decreased with the addition of oregano, bergamot, and cinnamon essential oils. Improvement of barrier characteristics against light, oxygen, and heat may be useful for long-term food preservation, despite the importance of transparency of films from the consumer's perspective. Light-sensitive food may benefit from the use of these films because of their ability to block UV rays and prevent oxidation (Zhou et al., 2021).

### 3.5. Colour

The colour of films or coatings used in food packaging is vital as it influences consumer acceptance (Jahdkaran et al., 2021). The data (Table 2) presented appears to be the results of colour measurements of coating solutions containing CTS, AVG, and varying concentrations of OPEO using  $L^*$   $a^*$   $b^*$  colour space. The data shows that the addition of OPEO is affecting the colour of the coating solution and making it more red, yellow and darker as the concentration of OPEO increases. Generally, CTS/AVG coating solution without OPEO exhibited slightly clear

Table 2

Colour analysis of CTS/AVG, CTS/AVG/1 %OPEO, CTS/AVG/2 %OPEO, CTS/AVG/3 %OPEO.

	$L^*$	$a^*$	$b^*$	$\Delta E$
CTS/AVG	$8.38 \pm 0.20^a$	$-0.59 \pm 0.22^{ab}$	$-0.64 \pm 0.03^c$	$51.93 \pm 0.08^c$
CTS/AVG/1 % OPEO	$6.97 \pm 0.16^b$	$-0.20 \pm 0.08^{ab}$	$-0.28 \pm 0.09^{bc}$	$53.18 \pm 0.18^b$
CTS/AVG/2 % OPEO	$6.72 \pm 0.33^b$	$-0.04 \pm 0.14^a$	$-0.06 \pm 0.07^b$	$53.40 \pm 0.33^b$
CTS/AVG/3 % OPEO	$5.10 \pm 0.20^c$	$0.17 \pm 0.28^a$	$1.01 \pm 0.37^a$	$54.57 \pm 0.23^a$

<sup>2</sup> Values in the same column with different superscript letters are significantly different ( $p < 0.05$ ).

Values are stated as mean  $\pm$  standard deviation,  $n = 3$ .

and transparent solution, however, the addition of OPEO, particularly at 3 % (v/w), significantly ( $P < 0.05$ ) declined the  $L^*$  (lightness) value from  $8.38 \pm 0.20$  to  $5.10 \pm 0.20$ , while the  $a^*$  (redness/greenness) and  $b^*$  values (yellowness) increased from  $-0.59 \pm 0.22$  to  $0.17 \pm 0.28$  and  $0.64 \pm 0.03$  to  $1.01 \pm 0.37$ , respectively, demonstrating a trend towards redness and yellowness ( $P < 0.05$ ).

This is consistent with the expected behaviour of OPEO, which is known to have high red and yellow pigments and can enhance the colour and appearance of the final product (Terzioğlu et al., 2021). It is also worth mentioning that  $\Delta E$  values of the coating solutions, which is a quantitative measurement of the colour difference, increased significantly with increasing OPEO levels as compared to the CTS/AVG coating solution ( $P < 0.05$ ), which is consistent with the visual observation of more difference in colour between each sample. Similar findings were reported by Li et al. (2021), where OPEO produced intrinsic yellow colour due to the damage of the carotenoids and flavonoids pigments in the orange peel. The developed coating solutions in this research incorporated with OPEO showed high  $b^*$  values and this could prevent nutrient losses, off-flavour and discolouration in packaged food by hindering visible and ultraviolet light.

### 3.6. FTIR analysis

The absorbance in the wavenumber region of  $4000\text{--}650\text{ cm}^{-1}$  at a resolution of  $4\text{ cm}^{-1}$  was measured using FTIR to assess the structural and spectroscopic changes in the formulated coating solution caused by the varied concentration of OPEO in CTS/AVG matrix. Fig. 6 displays the FTIR spectra of the different formulated coating solutions.

The shifts in the spectral peaks that occur during mixtures of different substances reflect the possible chemical interactions between the components of polymeric coating. From the results, the most prominent broad band was detected at  $3269.84\text{ cm}^{-1}$  in the spectrum signified the O-H stretching as all the materials used in the current research contains hydroxyl groups due to the dissolution of CTS in acetic

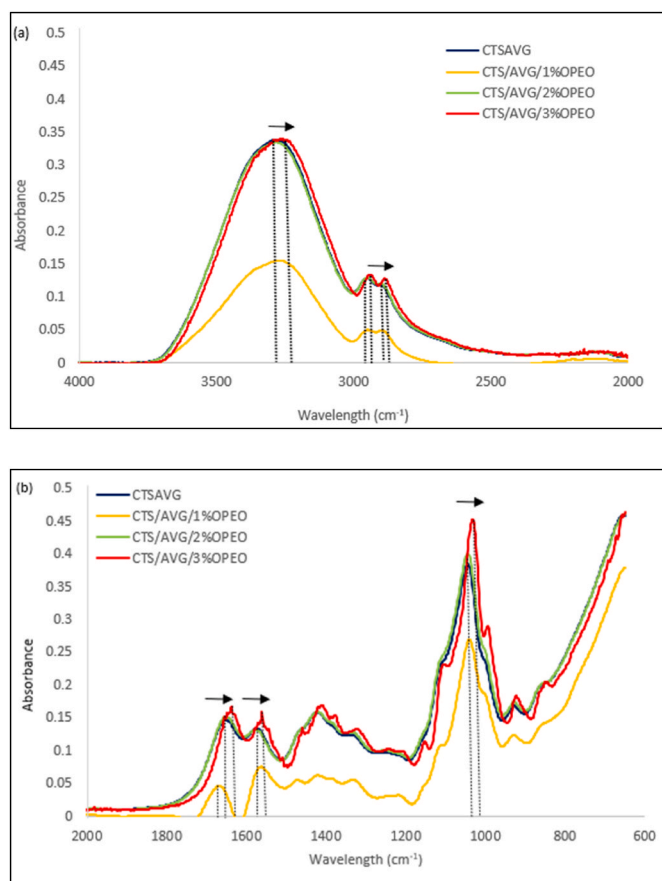


**Fig. 6.** Fourier transforms infrared analysis of CTS/AVG, CTS/AVG/1 %OPEO, CTS/AVG/2 %OPEO, CTS/AVG/3 %OPEO at wavelength of (a) 4000  $\text{cm}^{-1}$  to 2000  $\text{cm}^{-1}$  (b) 2000  $\text{cm}^{-1}$  to 600  $\text{cm}^{-1}$ .

acid as well as the presence of phenolic components found in AVG and OPEO (Sheikh et al., 2021). However, the peak at that wavelength region for CTS/AVG/1 %OPEO flattened probably owing to the chemical interactions of hydrogen bonding, hydrophobic forces or electrostatic interaction between CTS, AVG, and OPEO causing a decrease in stretching of free O-H bonds (Zheng et al., 2019).

The adjacent peaks found in the region of 2938–2885  $\text{cm}^{-1}$  were attributable to the C-H symmetric and asymmetric stretching as well as stretching of aliphatic -CH and -CH<sub>2</sub> groups (Anju et al., 2021). Meanwhile, a wavelength in a region of 1655–1630  $\text{cm}^{-1}$  ascribed vibrations of C=O bonds of the amide group RNHCO in CTS-based coating solution and carbonyl groups in AVG associated with acids, ketones and aldehydes (Yahya et al., 2022). In addition, 1655–1630  $\text{cm}^{-1}$  also corresponds to the carbonyl vibration of carboxylic acid of the remaining low volatile acetic acid used in dissolution of CTS. The reactive carbonyl and/or hydroxyl groups gives these biopolymers the ability to chemically interact with bioactive particles, which is a significant benefit (Bajer et al., 2020).

The FTIR spectra of CTS/AVG/OPEOs clearly demonstrates that numerous biomolecules of OPEO remained on the surface of the prepared CTS/AVG coating solution. Incorporation of OPEO in the polymeric matrix caused various small additional peaks in the wavelength range of 1500–1150  $\text{cm}^{-1}$  showing the various components found in essential oil. Distinct peaks of 1135–1105  $\text{cm}^{-1}$  and 1000–995  $\text{cm}^{-1}$  represent C-O stretching of terpenoid components and C=C bending vibrations of alkanes, respectively (Hasani et al., 2018; Benoudjit et al., 2020). Fig. 6 induced an increase in the concentration of OPEO causing a slight shift of the peaks to the right. This might probably be due to the increase of hydrogen bonding between those compounds and increase in

the functional groups of essential oil (Rambabu et al., 2019). Abral et al. (2021) pointed out that peak intensity variations, broadening of absorption peaks, and the emergence of new bands in the FTIR spectra all signified structural changes within the molecules or compounds.

### 3.7. Antioxidant properties

Antioxidants have been reported to play a crucial role in the prevention of numerous diseases associated with oxidative stress (Yahya et al., 2022). The antioxidant activities of CTS/AVG, CTS/AVG/1 % OPEO, CTS/AVG/2 %OPEO, and CTS/AVG/3 %OPEO were determined. According to Table 3 and Fig. 7, the antioxidant activity increased significantly with increasing concentration. As observed, the addition of OPEO to CTS/AVG increased the antioxidant potential in comparison to CTS/AVG alone, particularly at high concentration. Radical scavenging activities (RSA) demonstrated an increase in concentration of the coating solutions, and increased the radical scavenging activities of the coating solutions as shown in Fig. 7. IC<sub>50</sub> was recorded at 143.02 ± 0.54 mg/mL, 121.60 ± 0.72 mg/mL, 67.34 ± 0.47 mg/mL and 17.01 ± 0.45 mg/mL for CTS/AVG, CTS/AVG/1 %OPEO, CTS/AVG/2 %OPEO, and CTS/AVG/3 %OPEO, respectively.

Chitosan, aloe vera gel, and essential oils are widely acknowledged for their antioxidant and antimicrobial properties. Chitosan and aloe vera gel exhibit multiple antioxidant properties. Antioxidant activity of chitosan is predominantly due to its amino groups, which can effectively trap and neutralise free radicals by donating electrons, thereby reducing oxidative stress (Tamer et al., 2023). Free radicals are highly reactive molecules that can cause damage to cells and contribute to the development of numerous diseases. In addition to its antioxidant activity, chitosan has metal-chelating properties. It can bind to transition metal ions like iron and copper, preventing their participation in the Fenton and Haber-Weiss reactions that produce extremely reactive hydroxyl radicals. By chelating metal ions, chitosan inhibits metal-induced oxidative damage and reduces the formation of damaging free radicals (Grange et al., 2023). Similar to chitosan, aloe vera gel functions as a free radical scavenger and can boost endogenous antioxidant defences. Chitosan and aloe vera gel can stimulate the activity of antioxidant enzymes such as superoxide dismutase, catalase, and glutathione peroxidase, which play essential roles in neutralising reactive oxygen species, maintaining cellular redox balance, and protecting against oxidative stress (Mahgoob et al., 2023). Previous research by Yahya et al. (2022) confirmed that the aloe vera gel is a rich source of well-known antioxidant components by identifying and quantifying 13 phenolic and flavonoid chemicals. According to published research, phenolic component abundance is related to antioxidant performance.

**Table 3**

Antioxidant activity of CTS/AVG, CTS/AVG/1 %OPEO, CTS/AVG/2 %OPEO, and CTS/AVG/3 %OPEO.

Concentration (mg/mL)	Radical scavenging activity (%)			
	CTS/AVG	CTS/AVG/1 %OPEO	CTS/AVG/2 %OPEO	CTS/AVG/3 %OPEO
40	18.28 ± 0.26 <sup>d</sup>	19.01 ± 0.18 <sup>c</sup>	38.74 ± 0.08 <sup>b</sup>	53.93 ± 0.09 <sup>a</sup>
80	35.04 ± 0.08 <sup>d</sup>	41.80 ± 0.22 <sup>c</sup>	56.13 ± 0.14 <sup>b</sup>	62.99 ± 0.12 <sup>a</sup>
120	35.73 ± 0.75 <sup>d</sup>	54.92 ± 0.30 <sup>c</sup>	68.20 ± 0.15 <sup>b</sup>	77.54 ± 0.15 <sup>a</sup>
160	57.54 ± 0.50 <sup>d</sup>	62.00 ± 0.22 <sup>c</sup>	75.50 ± 0.20 <sup>b</sup>	85.27 ± 0.27 <sup>a</sup>
200	68.20 ± 0.26 <sup>d</sup>	69.83 ± 0.28 <sup>c</sup>	84.02 ± 0.09 <sup>b</sup>	88.84 ± 0.12 <sup>a</sup>
IC <sub>50</sub> (mg/mL)	143.02 ± 0.54 <sup>a</sup>	121.60 ± 0.72 <sup>b</sup>	67.34 ± 0.47 <sup>c</sup>	17.01 ± 0.45 <sup>d</sup>

<sup>2</sup> Values in the same row with different superscript letters are significantly different ( $p < 0.05$ ).

Values are stated as mean ± standard deviation,  $n = 3$ .



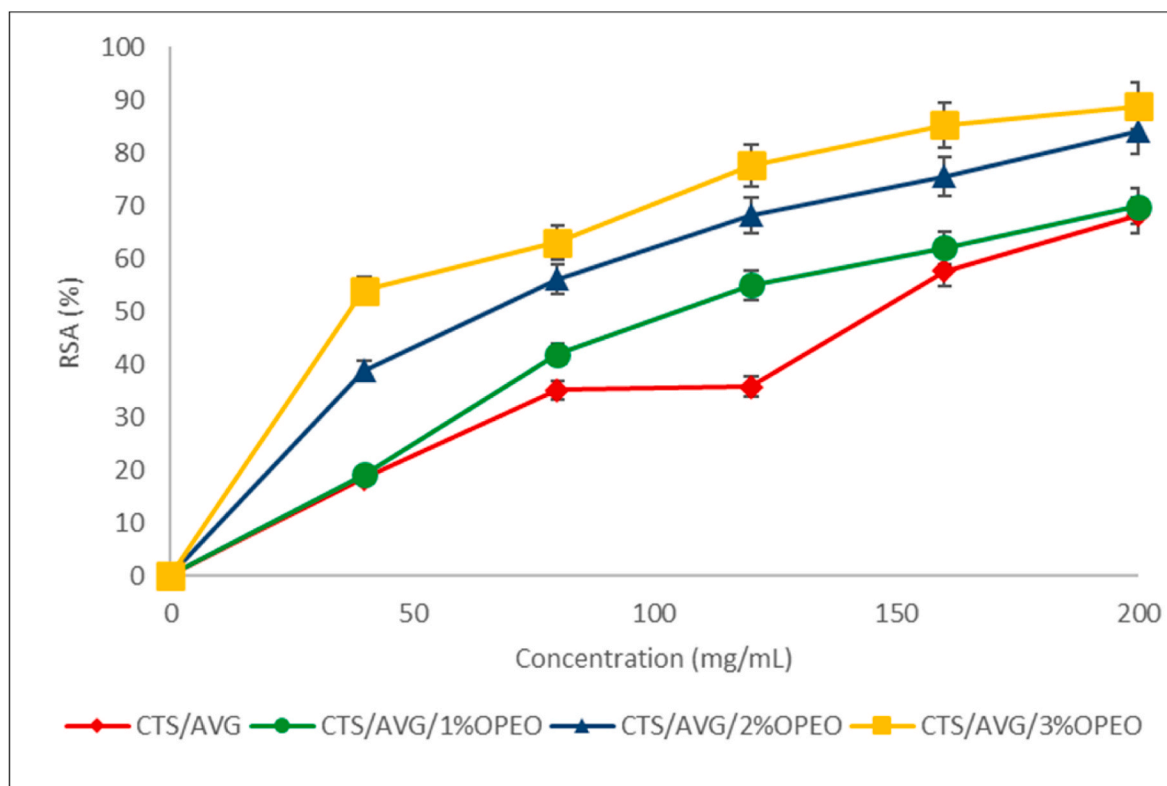


Fig. 7. Antioxidant activity of CTS/AVG, CTS/AVG/1 %OPEO, CTS/AVG/2 %OPEO, and CTS/AVG/3 %OPEO.

Due to their high concentration of phenolic compounds such as terpenes, phenols, and flavonoids, essential oils simultaneously manifest antioxidant activity. These compounds function as radical scavengers, neutralising and stabilising free radicals to protect cellular components from oxidative damage (Iordache et al., 2023). Additionally, essential oils can chelate metal ions, such as iron and copper, that are involved in the production of free radicals, thereby diminishing their detrimental effects (Yücel, 2021). Essential oils help maintain cellular health and minimise oxidative damage by reducing oxidative stress and protecting against free radicals. Addition of OPEO in the CTS/AVG matrix improved the antioxidant DPPH assay of the coating solutions due to the antioxidant activity present in OPEO.

### 3.8. Antibacterial properties

Antibacterial activity of coating solutions was measured in terms of inhibition zone (mm) against *Klebsiella pneumoniae*, *Pseudomonas*

**Table 4**  
Antimicrobial activity of CTS/AVG, CTS/AVG/1 %OPEO, CTS/AVG/2 %OPEO, and CTS/AVG/3 %OPEO against gram-positive and gram-negative bacteria.

Treatments	Zone of inhibition (mm)			
	Gram negative			Gram positive
	<i>Klebsiella pneumoniae</i>	<i>Pseudomonas aeruginosa</i>	<i>Escherichia coli</i>	<i>Staphylococcus aureus</i>
CTS/AVG	0 <sup>b</sup>	10.5 ± 1.3 <sup>b</sup>	0 <sup>c</sup>	0 <sup>b</sup>
CTS/AVG/1 %OPEO	0 <sup>b</sup>	10.5 ± 0.6 <sup>b</sup>	9.0 ± 0 <sup>b</sup>	10.5 ± 1.3 <sup>a</sup>
CTS/AVG/2 %OPEO	10.0 ± 0 <sup>a</sup>	12.0 ± 0.8 <sup>ab</sup>	9.5 ± 1.0 <sup>b</sup>	10.5 ± 1.9 <sup>a</sup>
CTS/AVG/3 %OPEO	10.0 ± 0.8 <sup>a</sup>	13.8 ± 0.5 <sup>a</sup>	14 ± 0.8 <sup>a</sup>	12.8 ± 0.5 <sup>a</sup>

<sup>2</sup> Values in the same column with different superscript letters are significantly different ( $p < 0.05$ ).

Values are stated as mean ± standard deviation, n = 3.

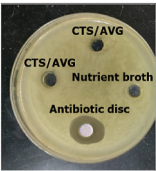
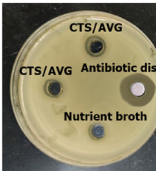
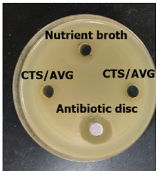
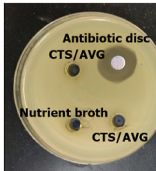
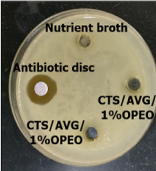
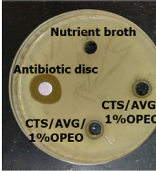
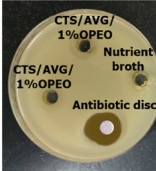
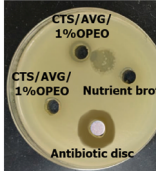
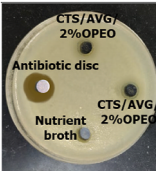
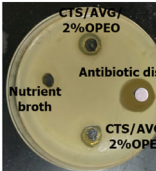
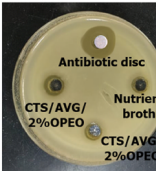
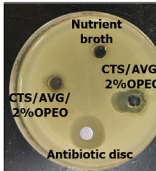
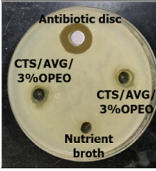
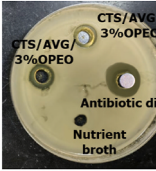
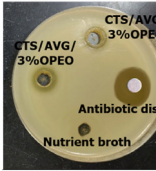

*aeruginosa*, *Escherichia coli*, and *Staphylococcus aureus* and presented in Table 4, Table 5 and Fig. 8. It is clearly shown that CTS/AVG only shows significant antimicrobial activity against *Pseudomonas aeruginosa* with an inhibition zone of  $10.5 \pm 1.3$  mm. There was no substantial bactericidal potential of aloe vera in the chitosan matrix, which may be because the bioactive components of aloe vera gel were trapped by the high concentration of chitosan (Iqbal et al., 2023). Incorporation of OPEO in CTS/AVG coating solutions increased the susceptibility of tested bacteria, thus increasing the zone of inhibition. CTS/AVG/3 % OPEO demonstrated the highest antimicrobial activity against *Klebsiella pneumoniae*, *Pseudomonas aeruginosa*, *Escherichia coli*, and *Staphylococcus aureus* with inhibition zones of  $10.0 \pm 0.8$  mm,  $13.8 \pm 0.5$  mm,  $14 \pm 0.8$  mm, and  $12.8 \pm 0.5$  mm, respectively.

The antimicrobial activity profile also showed that the prepared coating solution is more effective against gram-negative than gram-positive bacteria. Coating solution interacts with the lipid bilayer of gram-negative bacteria, resulting in cellular content leakage and cell viability impairment. The presence of lipopolysaccharides and protein in the outer membrane of gram-negative bacteria can interact with lipophilic substances, such as OPEO, thereby compromising the membrane's integrity and protective function (Okoye et al., 2023). Besides, gram-positive bacteria have thicker peptidoglycan layer as compared to gram-negative bacteria, therefore, making gram-positive bacteria less susceptible to the coating solution (Pokhrel et al., 2022). Antibacterial mechanisms of the coating solutions could be due to the electrostatic interaction between the coating molecules and microbial cell membranes that can lead to membrane disruption, intracellular component leakage, and eventual cell death (Fig. 9) (Hu et al., 2022).

Interaction of chitosan with microbial cell membranes confers antimicrobial properties. At physiological pH, chitosan possesses cationic properties, meaning it conveys a positive charge (Hua et al., 2021). As a result of the presence of phospholipids, microbial cell membranes typically bear a negative charge. This electrostatic interaction between positively charged chitosan and negatively charged phospholipids of

**Table 5**

Antibacterial activity of CTS/AVG, CTS/AVG/1 %OPEO, CTS/AVG/2 %OPEO, and CTS/AVG/3 %OPEO against gram-positive and gram-negative bacteria in well diffusion assay.

Inhibition zone of coating solutions				
<i>K. pneumoniae</i>	<i>P. aeruginosa</i>	<i>E. coli</i>	<i>S. aureus</i>	
<b>CTS/AVG</b>				
				
<b>CTS/AVG/1 %OPEO</b>				
				
<b>CTS/AVG/2 %OPEO</b>				
				
<b>CTS/AVG/3 %OPEO</b>				
				

microbial cell membranes can lead to membrane disruption, intracellular component leakage, and eventual cell death (Ke et al., 2022). Chitosan can also interfere with the enzyme systems of microorganisms, inhibiting essential cellular processes and microbial growth and replication. Moreover, metal-chelating properties of chitosan not only exhibit outstanding antioxidant properties, but also have positive antimicrobial effects. By disrupting microbial cell membranes and interfering with vital cellular functions, the complexation of chitosan with metal ions can enhance its antimicrobial activity (Zhang et al., 2022).

Aloe vera gel has broad-spectrum antimicrobial properties which can disrupt microbial cell membranes and inhibit critical microbial enzymes. It causes membrane permeabilization and leakage of cellular contents by penetrating the cell walls of microorganisms. Additionally, aloe vera gel contains compounds that inhibit key microbial enzymes involved in cell wall synthesis, protein synthesis, and energy metabolism, thereby inhibiting microbial growth and replication. In addition, aloe vera gel stimulates the immune system, boosting the activity of immune cells such as macrophages and lymphocytes to combat microbial infections (Darzi et al., 2021).

Essential oils, chitosan, and aloe vera gel, possess antimicrobial activity by disrupting microbial cell membranes via their lipophilicity and

volatile constituents. They are capable of penetrating and disrupting the lipid bilayer of microbial membranes, resulting in cell death. Furthermore, essential oils inhibit microbial growth and replication by interfering with vital cellular processes such as protein synthesis, DNA replication, and cell wall synthesis. In addition, they can modulate the expression of microbial genes involved in virulence and pathogenesis, thereby reducing the ability of microorganisms to cause infections, and boosting the efficacy of the immune response against them (Hu et al., 2022).

#### 4. Conclusion

This study successfully incorporated orange peel essential oil (OPEO) into the chitosan/Aloe vera matrix (CTS/AVG). With the addition of OPEO, particle size decreased and Brownian motion increased, indicating enhanced dispersion within the matrix. Moreover, the consistent stability of the emulsions across different concentrations of OPEO suggests that OPEO is effectively dispersed within the CTS/AVG matrix. Besides, the combination of CTS/AVG and OPEO in the coating solution led to notable changes in viscosity, pH, and density. The variations were influenced by the cross-linked interaction between these components. In

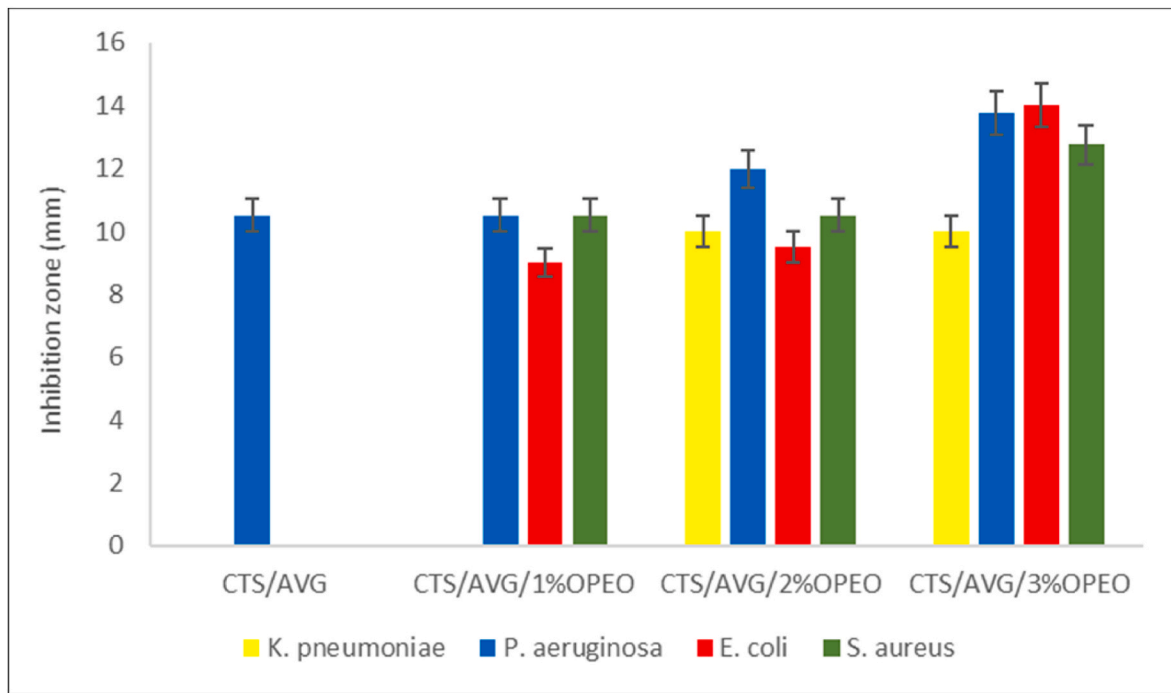


Fig. 8. Antimicrobial activity of CTS/AVG, CTS/AVG/1 %OPEO, CTS/AVG/2 %OPEO, and CTS/AVG/3 %OPEO against gram-positive and gram-negative bacteria.

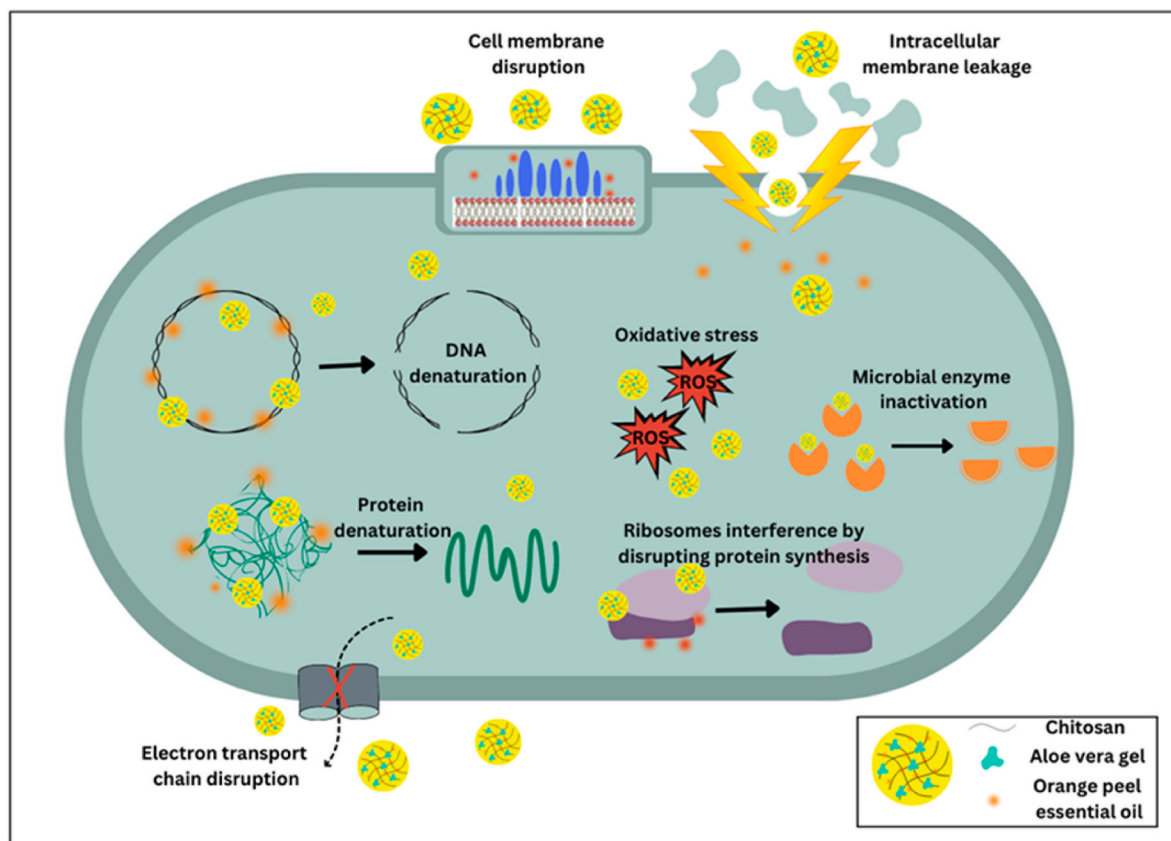


Fig. 9. Preservation mechanisms of coating solution.

addition, the incorporation of OPEO into CTS/AVG reduced the water vapour transmission rate and diffusion coefficient significantly as an increase in OPEO concentration caused an increase in hydrophobicity and thus decreased the moisture barrier. Additionally, the incorporation

of OPEO significantly improved UV-Vis shielding in the CTS/AVG coating solutions, with 3 % OPEO showing the highest UV-blocking capacity. Addition of OPEO also shifted the coating solutions towards red and yellow hues, enhancing their appearance and potential to

preserve light-sensitive foods and prevent nutrient loss and off-flavours. Furthermore, FTIR analysis of the coating solutions demonstrated significant spectral shifts and additional peaks, indicating chemical interactions among chitosan, aloe vera gel, and orange peel essential oil (OPEO). The changes in peak intensities and shifts, particularly in the O-H stretching and C-O stretching regions, reflect structural modifications and interactions within the coating solution caused by OPEO incorporation. The coating solution containing 3 % OPEO displayed the greatest antioxidant activity, as evidenced by its superior DPPH radical scavenging effect and lowest IC<sub>50</sub> value. In addition, the antimicrobial analysis revealed that the coating solutions were more effective against gram-positive bacteria than gram-negative bacteria, with CTS/AVG/3 % OPEO exhibiting the greatest inhibition against *E. coli*. Overall, these results demonstrate that CTS/AVG/3 %OPEO has the potential to serve as a natural alternative to synthetic preservatives in the fruit industry, as it possesses outstanding physicochemical properties.

### Funding sources

This work was supported by the Universiti Malaysia Sabah GUG0558-1/2022.

### CRedit authorship contribution statement

**Wen Xia Ling Felicia:** The authors' contribution as stated. **Rovina Kobun:** did the, Formal analysis, experimentation and wrote the main manuscript text. **Nasir Md Nur Aqilah:** supervised, reviewed, and edited the main manuscript text. **Sylvester Mantihal:** conceived, participated and designed the work. **Nurul Huda:** conceived, participated and designed the work.

### Declaration of competing interest

The authors declare the following financial interests/personal relationships which may be considered as potential competing interests:

Kobun Rovina reports financial support and article publishing charges were provided by University of Malaysia Sabah Faculty of Food Science and Nutrition.

### Data availability

No data was used for the research described in the article.

### Acknowledgements

Conceptualization: W.X.L.F. and K.R.; resourcing and writing—original draft preparation: K.R., W.X.L.F., M.N.N., S.M. and N.H.; writing—review and editing: K.R., W.X.L.F., and S.M.; supervision: K.R. All authors have read and agreed to the published version of the manuscript.

### References

- Abral, H., Pratama, A.B., Handayani, D., Mahardika, M., Aminah, I., Sandrawati, N., Sugiarti, E., Muslimin, A.N., Sapuan, S.M., Ilyas, R.A., 2021. Antimicrobial edible film prepared from bacterial cellulose nanofibers/starch/chitosan for a food packaging alternative. *Int. J. Polym. Sci.* 2021, 1–11. <https://doi.org/10.1155/2021/6641284>.
- Ajaz, N., Bukhsh, M., Kamal, Y., Rehman, F., Irfan, M., Khalid, S.H., Asghar, S., Rizg, W. Y., Bukhary, S.M., Hosny, K.M., Alissa, M., 2023. Development and evaluation of pH sensitive semi-interpenetrating networks: assessing the impact of itaconic acid and aloe vera on network swelling and cetrizine release. *Front. Bioeng. Biotechnol.* 11, 1173883 <https://doi.org/10.3389/fbioe.2023.1173883>.
- Akarca, G., Sevik, R., 2021. Biological Activities of Citrus limon L. and Citrus sinensis L. Peel essential oils. *Journal of Essential Oil Bearing Plants* 24 (6), 1415–1427. <https://doi.org/10.1080/0972060X.2021.2022000>.
- Algharib, S.A., Dawood, A., Zhou, K., Chen, D., Li, C., Meng, K., Zhang, A., Luo, W., Ahmed, S., Huang, L., Xie, S., 2022. Preparation of chitosan nanoparticles by ionotropic gelation technique: effects of formulation parameters and in vitro

- characterization. *J. Mol. Struct.* 1252, 132129 <https://doi.org/10.1016/j.molstruc.2021.132129>.
- Ali, M.R., Yousef, A., Ali, A., 2021. Application of Biodegradable Aloe vera gel and Linseed mucilage for extending the shelf life of Plums. *Res. J. Pharm. Technol.* 14, 1579–1585. <https://doi.org/10.5958/0974-360X.2021.00279.1>.
- Alkaabi, S., Sobti, B., Mudgil, P., Hasan, F., Ali, A., Nazir, A., 2022. Lemongrass essential oil and Aloe vera gel based antimicrobial coatings for date fruits. *Appl. Food Res.* 100127 <https://doi.org/10.1016/j.afres.2022.100127>.
- Amin, U., Khan, M.K.I., Khan, M.U., Ehtasham Akram, M., Pateiro, M., Lorenzo, J.M., Maan, A.A., 2021. Improvement of the performance of chitosan—aloe vera coatings by adding beeswax on postharvest quality of mango fruit. *Foods* 10, 2240. <https://doi.org/10.3390/foods10102240>.
- ASTM, A., 2013. D1653-13: Standard Test Methods for Water Vapor Transmission of Organic Coating Films. ASTM International, West Conshohocken, PA, USA.
- Azman, M.A., Asyraf, M.R.M., Khalina, A., Petri, M., Ruzaidi, C.M., Sapuan, S.M., Wan Nik, W.B., Ishak, M.R., Ilyas, R.A., Suriani, M.J., 2021. Natural fiber reinforced composite material for product design: a short review. *Polym* 13, 1917. <https://doi.org/10.3390/polym13121917>.
- Azmin, S.N.H.M., Nor, M.S.M., 2020. Development and characterization of food packaging bioplastic film from cocoa pod husk cellulose incorporated with sugarcane bagasse fibre. *J. Bioresour. Bioprod.* 5 (4), 248–255. <https://doi.org/10.1016/j.jobab.2020.10.003>.
- Bajer, D., Janczak, K., Bajer, K., 2020. Novel starch/chitosan/aloe vera composites as promising biopackaging materials. *J. Polym. Environ.* 28, 1021–1039. <https://doi.org/10.1007/s10924-020-01661-7>.
- Benoudjit, F., Maameri, L., Ouared, K., 2020. Evaluation of the quality and composition of lemon (*Citrus limon*) peel essential oil from an Algerian fruit juice industry. *Algerian Journal of Environmental Science and Technology* 6.
- Bhaskar, R., Zo, S.M., Kanan, B.N., Purohit, S., Gupta, M.K., Han, S.S., 2023. Recent development of protein-based biopolymers in food packaging applications: a review. *Polym. Test.*, 108097 <https://doi.org/10.1016/j.polymertesting.2023.108097>.
- Bitterling, H., Mailänder, L., Vetter, W., Kammerer, D.R., Stintzing, F.C., 2022. Photoprotective effects of furocoumarins on terpenes in lime, lemon and bergamot essential oils upon UV light irradiation. *Eur. Food Res. Technol.* 248, 1049–1057. <https://doi.org/10.1007/s00217-021-03945-1>.
- Cheng, H., Khan, M.A., Xie, Z., Tao, S., Li, Y., Liang, L., 2020. A peppermint oil emulsion stabilized by resveratrol-zein-pectin complex particles: enhancing the chemical stability and antimicrobial activity in combination with the synergistic effect. *Food Hydrocolloids* 103, 105675. <https://doi.org/10.1016/j.foodhyd.2020.105675>.
- Chowdhury, S., Teoh, Y.L., Ong, K.M., Zaidi, N.S.R., Mah, S.K., 2020. Poly (vinyl) alcohol crosslinked composite packaging film containing gold nanoparticles on shelf life extension of banana. *Food Packag. Shelf Life* 24, 100463. <https://doi.org/10.1016/j.fpsl.2020.100463>.
- Ćirin, D., Pavlović, N., Nikolić, I., Krstonosić, V., 2023. Assessment of soy protein acid hydrolysate—xanthan gum mixtures on the stability, disperse and rheological properties of oil-in-water emulsions. *Polym* 15, 2195. <https://doi.org/10.3390/polym15092195>.
- Darzi, S., Paul, K., Leitan, S., Werkmeister, J.A., Mukherjee, S., 2021. Immunobiology and application of aloe vera-based scaffolds in tissue engineering. *Int. J. Mol. Sci.* 22 (4), 1708. <https://doi.org/10.3390/ijms22041708>.
- De Matteis, V., Cascione, M., Costa, D., Martano, S., Manno, D., Cannavale, A., Mazzotta, S., Paladini, F., Martino, M., Rinaldi, R., 2023. Aloe vera silver nanoparticles addition in chitosan films: improvement of physicochemical properties for eco-friendly food packaging material. *J. Mater. Res. Technol.* 24, 1015–1033. <https://doi.org/10.1016/j.jmrt.2023.03.025>.
- Diyana, Z.N., Jumaidin, R., Selamat, M.Z., Ghazali, I., Julmohammad, N., Huda, N., Ilyas, R.A., 2021. Physical properties of the thermoplastic starch derived from natural resources and its blends: a review. *Polym* 13, 1396. <https://doi.org/10.3390/polym13091396>.
- Duan, C., Meng, X., Meng, J., Khan, M.I.H., Dai, L., Khan, A., An, X., Zhang, J., Huq, T., Ni, Y., 2019. Chitosan as a preservative for fruits and vegetables: a review on chemistry and antimicrobial properties. *J. Bioresour. Bioprod.* 4, 11–21. <https://doi.org/10.21967/jbb.v4i1.189>.
- Ernesto, J.V., de Macedo Gasparini, Í., Corazza, F.G., Mather, M.B., da Silva, C.F., Leite-Silva, V.R., Andréo-Filho, N., Lopes, P.S., 2023. Physical, chemical, and biological characterization of biodegradable chitosan dressing for biomedical applications: could sodium bicarbonate act as a crosslinking agent? *Mater. Chem. Phys.* 301, 127636 <https://doi.org/10.1016/j.matchemphys.2023.127636>.
- Esmaili, Y., Zamindar, N., Paidari, S., Ibrahim, S.A., Mohammadi Nafchi, A., 2021. The synergistic effects of aloe vera gel and modified atmosphere packaging on the quality of strawberry fruit. *J. Food Process. Preserv.* 45, e16003 <https://doi.org/10.1111/jfpp.16003>.
- Felicia, W.X.L., Rovina, K., Nur'Aqilah, M.N., Vonnice, J.M., Erna, K.H., Misson, M., Halid, N.F.A., 2022a. Recent advancements of polysaccharides to enhance quality and delay ripening of fresh produce: a review. *Polym* 14, 1341. <https://doi.org/10.3390/polym14071341>.
- Felicia, W.X.L., Rovina, K., Vonnice, J.M., Aqilah, M.N.N., Erna, K.H., Mailin, M., 2022b. Consolidating plant-based essential oils onto polysaccharides-based coatings: effect on mechanisms and reducing postharvest losses of fruits. *Appl. Food Res.* 100226 <https://doi.org/10.1016/j.afres.2022.100226>.
- Grange, C., Aigle, A., Ehrlich, V., Salazar Ariza, J.F., Brichart, T., Da Cruz-Boisson, F., David, L., Lux, F., Tillement, O., 2023. Design of a water-soluble chitosan-based polymer with antioxidant and chelating properties for labile iron extraction. *Sci. Rep.* 13, 7920. <https://doi.org/10.1038/s41598-023-34251-3>.
- Gupta, S., Sani, A., Laodheerasiri, S., Chuenchom, L., Watcharin, W., 2023. Nanoencapsulated grapefruit essential oil with carrageenan: facile preparation,

- characterization and cytotoxicity studies. In: AIP Conference Proceedings. AIP Publishing. <https://doi.org/10.1063/5.0136867>.
- Hasani, S., Ojagh, S.M., Ghorbani, M., 2018. Nanoencapsulation of lemon essential oil in Chitosan-Hicap system. Part I: study on its physical and structural characteristics. *Int. J. Biol. Macromol.* 115, 143–151. <https://doi.org/10.1016/j.ijbiomac.2018.04.038>.
- Hasheminya, S.M., Mokarram, R.R., Ghanbarzadeh, B., Hamishekar, H., Kafil, H.S., Dehghannya, J., 2019. Influence of simultaneous application of copper oxide nanoparticles and *Satureja Khuzestanica* essential oil on properties of kefirán-carboxymethyl cellulose films. *Polym. Test.* 73, 377–388. <https://doi.org/10.1016/j.polymertesting.2018.12.002>.
- Hu, Z., Lu, C., Zhang, Y., Tong, W., Du, L., Liu, F., 2022. Proteomic analysis of *Aspergillus flavus* reveals the antifungal action of *Perilla frutescens* essential oil by interfering with energy metabolism and defense function. *Lwt* 154, 112660. <https://doi.org/10.1016/j.lwt.2021.112660>.
- Hua, Y., Wei, Z., Xue, C., 2021. Chitosan and its composites-based delivery systems: advances and applications in food science and nutrition sector. *Crit. Rev. Food Sci. Nutr.* 1–20. <https://doi.org/10.1080/10408398.2021.2004992>.
- Huang, G., Lai, B., Xu, H., Jin, Y., Huo, L., Li, Z., Deng, Y., 2021. Fabrication of a superhydrophobic fabric with a uniform hierarchical structure via a bottom-blown stirring method for highly efficient oil–water separation. *Sep. Purif. Technol.* 258, 2768–2778. <https://doi.org/10.1016/j.seppur.2020.118063>.
- Iordache, A.M., Nechita, C., Podea, P., Şuvar, N.S., Mesaroş, C., Voica, C., Culea, M., 2023. Comparative amino acid profile and antioxidant activity in sixteen plant extracts from transylvania, Romania. *Plants* 12, 2183. <https://doi.org/10.3390/plants12112183>.
- Iqbal, D.N., Munir, A., Abbas, M., Nazir, A., Ali, Z., Alshawwa, S.Z., Iqbal, M., Ahmad, N., 2023. Polymeric membranes of chitosan/aloë vera gel fabrication with enhanced swelling and antimicrobial properties for biomedical applications. *Dose Response* 21, 15593258231169387. <https://doi.org/10.1177/15593258231169387>.
- Jahdkaran, E., Hosseini, S.E., Mohammadi Nafchi, A., Nouri, L., 2021. The effects of methylcellulose coating containing carvacrol or menthol on the physicochemical, mechanical, and antimicrobial activity of polyethylene films. *Food Sci. Nutr.* 9, 2768–2778. <https://doi.org/10.1002/fsn3.2240>.
- Jia, Z., Li, J., Gao, L., Yang, D., Kanaev, A., 2023. Dynamic light scattering: a powerful tool for in situ nanoparticle sizing. *Colloids and Interfaces* 7, 15. <https://doi.org/10.3390/colloids7010015>.
- Ke, Y., Ding, B., Zhang, M., Dong, T., Fu, Y., Lv, Q., Ding, W., Wang, X., 2022. Study on inhibitory activity and mechanism of chitosan oligosaccharides on *Aspergillus Flavus* and *Aspergillus Fumigatus*. *Carbohydr. Polym.* 275, 118673. <https://doi.org/10.1016/j.carbpol.2021.118673>.
- Kohli, S.K., Bali, S., Tejpal, R., Bhalla, V., Verma, V., Bhardwaj, R., Alqarawi, A.A., Abd Allah, E.F., Ahmad, P., 2019. In-situ localization and biochemical analysis of bio-molecules reveals Pb-stress amelioration in *Brassica juncea* L. by co-application of 24-Epibrassinolide and Salicylic Acid. *Sci. Rep.* 9, 3524. <https://doi.org/10.1038/s41598-019-39712-2>.
- La, D.D., Nguyen-Tri, P., Le, K.H., Nguyen, P.T., Nguyen, M.D.B., Vo, A.T., Nguyen, M.T., Chang, S.W., Tran, L.D., Chung, W.J., Nguyen, D.D., 2021. Effects of antibacterial ZnO nanoparticles on the performance of a chitosan/gum Arabic edible coating for post-harvest banana preservation. *Prog. Org. Coating* 151, 106057. <https://doi.org/10.1016/j.porgcoat.2020.106057>.
- Lastra Ripoll, S.E., Quintana Martinez, S.E., Garcia Zapateiro, L.A., 2021. Rheological and microstructural properties of xanthan gum-based coating solutions enriched with phenolic mango (*Mangifera indica*) peel extracts. *ACS Omega* 6 (24), 16119–16128. <https://doi.org/10.1021/acsomega.1c02011>.
- Li, Y., Tang, C., He, Q., 2021. Effect of orange (*Citrus sinensis* L.) peel essential oil on characteristics of blend films based on chitosan and fish skin gelatin. *Food Biosci.* 41, 100927. <https://doi.org/10.1016/j.fbio.2021.100927>.
- Liguori, G., Gaglio, R., Settanni, L., Inglese, P., D'Anna, F., Miceli, A., 2021. Effect of opuntia ficus-indica mucilage edible coating in combination with ascorbic acid, on strawberry fruit quality during cold storage. *J. Food Qual.* <https://doi.org/10.1155/2021/9976052>, 2021.
- Mahajan, K., Kumar, S., Bhat, Z.F., Naqvi, Z., Mungure, T.E., Bekhit, A.E.D.A., 2021. Functionalization of carrageenan based edible film using Aloe vera for improved lipid oxidative and microbial stability of frozen dairy products. *Food Biosci.* 43, 101336. <https://doi.org/10.1016/j.fbio.2021.101336>.
- Mahcene, Z., Khelil, A., Hasni, S., Akman, P.K., Bozkurt, F., Birech, K., Goudjil, M.B., Tornuk, F., 2020. Development and characterization of sodium alginate based active edible films incorporated with essential oils of some medicinal plants. *Int. J. Biol. Macromol.* 145, 124–132. <https://doi.org/10.1016/j.ijbiomac.2019.12.093>.
- Mahgoub, A.A.E., Tousson, E., Abd Eldaim, M.A., Ullah, S., Al-Sehemi, A.G., Algarni, H., El Sayed, I.E.T., 2023. Ameliorative role of chitosan nanoparticles against silver nanoparticle-induced reproductive toxicity in male albino rats. *Environ. Sci. Pollut. Res.* 30, 17374–17383. <https://doi.org/10.1007/s11356-022-23312-1>.
- Mohammadi, L., Khankahdani, H.H., Tanaka, F., Tanaka, F., 2021. Postharvest shelf-life extension of button mushroom (*Agaricus bisporus* L.) by Aloe vera gel coating enriched with basil essential oil. *Environ. Control Biol.* 59, 87–98. <https://doi.org/10.2525/ecb.59.87>.
- Nogueira, G.F., Fakhouri, F.M., de Oliveira, R.A., 2019. Effect of incorporation of blackberry particles on the physicochemical properties of edible films of arrowroot starch. *Dry. Technol.* 37, 448–457. <https://doi.org/10.1080/07379397.2018.1441153>.
- Nourozi, F., Sayyari, M., 2020. Enrichment of Aloe vera gel with basil seed mucilage preserve bioactive compounds and postharvest quality of apricot fruits. *Sci. Hortic.* 262, 109041. <https://doi.org/10.1016/j.scienta.2019.109041>.
- Okoye, C.O., Okeke, E.S., Ezeorba, T.P.C., Chukwudozie, K.I., Chiejina, C.O., Fomena Temgoua, N.S., 2023. Microbial and bio-based preservatives: recent advances in antimicrobial compounds. *Microbes for natural food additives* 53–74. [https://doi.org/10.1007/978-981-19-5711-6\\_4](https://doi.org/10.1007/978-981-19-5711-6_4).
- Padilla-de la Rosa, J.D., Manzano-Alfaro, M.D., Gómez-Huerta, J.R., Arriola-Guevara, E., Guatemala-Morales, G., Cardador-Martínez, A., Estarrón-Espinosa, M., 2021. Innovation in a continuous system of distillation by steam to obtain essential oil from Persian lime juice (*Citrus latifolia tanaka*). *Mol* 26, 4172. <https://doi.org/10.3390/molecules26144172>.
- Panda, P.K., Sadeghi, K., Seo, J., 2022. Recent advances in poly (vinyl alcohol)/natural polymer based films for food packaging applications: a review. *Food Packag. Shelf Life* 33, 100904. <https://doi.org/10.1016/j.fpsl.2022.100904>.
- Pavoni, J.M.F., Luchese, C.L., Tessaro, I.C., 2019. Impact of acid type for chitosan dissolution on the characteristics and biodegradability of cornstarch/chitosan based films. *Int. J. Biol. Macromol.* 138, 693–703. <https://doi.org/10.1016/j.ijbiomac.2019.07.089>.
- Peng, Y., Li, Y., 2014. Combined effects of two kinds of essential oils on physical, mechanical and structural properties of chitosan films. *Food Hydrocolloids* 36, 287–293. <https://doi.org/10.1016/j.foodhyd.2013.10.013>.
- Pokhrel, R., Shakya, R., Baral, P., Chapagain, P., 2022. Molecular modeling and simulation of the peptidoglycan layer of gram-positive bacteria *Staphylococcus aureus*. *J. Chem. Inf. Model.* 62, 4955–4962. <https://doi.org/10.1021/acs.jcim.2c00437>.
- Qiao, G., Xiao, Z., Ding, W., Rok, A., 2019. Effect of chitosan/nano-titanium dioxide/thymol and tween films on ready-to-eat cantaloupe fruit quality. *Coatings* 9, 828. <https://doi.org/10.3390/coatings9120828>.
- Rambabu, K., Bharath, G., Banat, F., Show, P.L., Cocolozzi, H.H., 2019. Mango leaf extract incorporated chitosan antioxidant film for active food packaging. *Int. J. Biol. Macromol.* 126, 1234–1243. <https://doi.org/10.1016/j.ijbiomac.2018.12.196>.
- Sathiyaraj, S., Suriyakala, G., Gandhi, A.D., Babujanarathanam, R., Almaary, K.S., Chen, T.W., Kaviyarasu, K., 2021. Biosynthesis, characterization, and antibacterial activity of gold nanoparticles. *J. Infect. Public Health.* 14, 1842–1847. <https://doi.org/10.1016/j.jiph.2021.10.007>.
- Shebis, Y., Laskavy, A., Molad-Filosof, A., Arnon-Rips, H., Natan-Warhaftig, M., Jacobi, G., Fallik, E., Banin, E., Poverenov, E., 2022. Non-radical synthesis of chitosan-quercetin polysaccharide: properties, bioactivity and applications. *Carbohydr. Polym.* 284, 119206. <https://doi.org/10.1016/j.carbpol.2022.119206>.
- Sheikh, M., Mehnaz, S., Sadiq, M.B., 2021. Prevalence of fungi in fresh tomatoes and their control by chitosan and sweet orange (*Citrus sinensis*) peel essential oil coating. *J. Sci. Food Agric.* 101, 6248–6257. <https://doi.org/10.1002/jsfa.11291>.
- Shen, Y., Ni, Z.J., Thakur, K., Zhang, J.G., Hu, F., Wei, Z.J., 2021. Preparation and characterization of clove essential oil loaded nanoemulsion and pickering emulsion activated pullulan-gelatin based edible film. *Int. J. Biol. Macromol.* 181, 528–539. <https://doi.org/10.1016/j.ijbiomac.2021.03.133>.
- Soltani, M., Kashkooli, F.M., Fini, M.A., Gharapetian, D., Nathwani, J., Dusseault, M.B., 2022. A review of nanotechnology fluid applications in geothermal energy systems. *Renew. Sust. Energ. Rev.* 167, 112729. <https://doi.org/10.1016/j.rser.2022.112729>.
- Tamer, T.M., ElTantawy, M.M., Brussevich, A., Nebalueva, A., Novikov, A., Moskalenko, I.V., Skorb, E.V., 2023. Functionalization of chitosan with poly aromatic hydroxyl molecules for improving its antibacterial and antioxidant properties: practical and theoretical studies. *Int. J. Biol. Macromol.* 234, 123687. <https://doi.org/10.1016/j.ijbiomac.2023.123687>.
- Terzioğlu, P., Güneş, F., Parn, F.N., Şen, İ., Tuna, S., 2021. Biowaste orange peel incorporated chitosan/polyvinyl alcohol composite films for food packaging applications. *Food Packag. Shelf Life* 30, 100742. <https://doi.org/10.1016/j.fpsl.2021.100742>.
- TsegayeFekadu, T.S., Abera, A., 2019. Extraction of essential oil from orange peel using different methods and effect of solvents, time, temperature to maximize yield. *Int. J. Eng. Sci.* 9, 24300–24308.
- Wang, J., Zhuang, S., 2022. Chitosan-based materials: preparation, modification and application. *J. Clean. Prod.* 355, 131825. <https://doi.org/10.1016/j.jclepro.2022.131825>.
- Yahya, R., Al-Rajhi, A.M., Alzaid, S.Z., Al Abboud, M.A., Almuhayawi, M.S., Al Jaouni, S. K., Selim, S., Ismail, K.S., Abdelghany, T.M., 2022. Molecular docking and efficacy of aloe vera gel based on chitosan nanoparticles against *Helicobacter pylori* and its antioxidant and anti-inflammatory activities. *Polym* 14, 2994. <https://doi.org/10.3390/polym14152994>.
- Yücel, T.B., 2021. Chemical composition and antimicrobial and antioxidant activities of essential oils of *Polytrichum commune* (Hedw.) and *Antitrichia curtispindula* (Hedw.) Brid. grown in Turkey. *Int. J. Second. Metab.* 8, 272–282. <https://doi.org/10.21448/ijsm.945405>.
- Zhang, W., Liu, D., Fu, X., Xiong, C., Nie, Q., 2022. Peel essential oil composition and antibacterial activities of *Citrus x sinensis* L. Osbeck 'arococco' and *Citrus reticulata* blanco. *Horticulture* 8, 793. <https://doi.org/10.3390/horticulture8090793>.
- Zheng, H., Rao, J., 2023. Nanoemulsions and emulsions. In: *Bioactive Delivery Systems for Lipophilic Nutraceuticals: Formulation, Fabrication, and Application*. The Royal Society of Chemistry.
- Zheng, K., Xiao, S., Li, W., Wang, W., Chen, H., Yang, F., Qin, C., 2019. Chitosan-acorn starch-eugenol edible film: physico-chemical, barrier, antimicrobial, antioxidant and structural properties. *Int. J. Biol. Macromol.* 135, 344–352. <https://doi.org/10.1016/j.ijbiomac.2019.05.151>.
- Zhou, Y., Wu, X., Chen, J., He, J., 2021. Effects of cinnamon essential oil on the physical, mechanical, structural and thermal properties of cassava starch-based edible films. *Int. J. Biol. Macromol.* 184, 574–583. <https://doi.org/10.1016/j.ijbiomac.2021.06.067>.